Crystal Structure of Zeolite MCM-35 (MTF)

Philip A. Barrett, María-José Díaz-Cabañas, and Miguel A. Camblor*

Instituto de Tecnología Química (C.S.I.C.-U.P.V.), Universidad Politécnica de Valencia, Avda. Los Naranjos s/n, 46022 Valencia, Spain

Received May 17, 1999. Revised Manuscript Received July 15, 1999

Zeolite MCM-35 may be crystallized in its pure silica form in fluoride or hydroxide media at relatively low pH (below 11) in the presence of hexamethyleneimine. Its crystal structure has been solved by direct methods and refined using synchrotron powder diffraction data. Calcined MCM-35, $[Si_{44}O_{88}]$, has a new zeolite topology (monoclinic, space group $C2/m$, a = 9.49998 Å, b = 30.7096 Å, c = 7.31333 Å, β = 91.7113°) and contains small one-dimensional pores with openings defined by windows of eight tetrahedra.

Introduction

Synthetic efforts during the last 40 years have produced a large number of zeolites, and around 100 different zeolite topologies have been determined.[1] It is notable that most of the new zeolites discovered recently have been synthesized by the use of relatively complex and sophisticated organic cations employed as structure-directing agents (SDA). This synthetic approach mainly relies on the believe that new zeolites require rather specific SDA to be used, since zeolites that need little structure-direction specificity (which have been called "default host lattices")[2] should have already appeared over all these years of synthetic effort. The specificity of the SDA, which most frequently are organoammonium cations, has been related to properties such as conformational rigidity, size and hydrophobicity (characterized by the C/N^+ ratio).[3] While this approach has proved extremely fruitful over the past few years, it is interesting to note that some new, recently discovered zeolites (such as MCM-22[4] and MCM-35)[5] have been synthesized by using an amine (hexamethyleneimine) with a relatively low conformational rigidity (single cycle amine), a small size, and, when protonated, a low C/N^+ ratio of 6, well below those considered optimum for synthesizing highly siliceous zeolites (C/N^+= 11−15).[3] It is somehow surprising that it is still possible to discover new high silica zeolites by using small and flexible organic additives.

To understand the synthesis and properties of zeolites and to identify their potential applications, the determination of their topologies is of great importance. In addition to the difficulties inherent to the determination of crystal structures by powder diffraction techniques, zeolites presenting poor adsorption properties may not receive adequate attention because of their possibly limited commercial interest. This may be true in the case of zeolite MCM-35, a material which has received no attention in the literature since its first patent report (1991),[5] most probably due to its very small micropore volume. However, from the viewpoint of zeolite chemistry, such materials may have the same importance as those presenting more commercially appealing properties. We therefore initiated the study of MCM-35 and succeded in synthesizing materials with a pure SiO_2 composition. It was noted that by varying the synthesis conditions the X-ray powder diffraction patterns, which typically contain some rather broad reflections, may be greatly improved. This allowed us to solve the structure by direct methods using synchrotron X-ray diffraction data. MCM-35 is a zeolite containing a one-dimensional small pore channel, with minimum apertures defined by windows containing eight $SiO_{4/2}$ tetrahedra (8MR channel).

Experimental Section

We have synthesized pure silica MCM-35 materials under a number of different conditions (Table 1), always in the presence of hexamethyleneimine (HMI). The synthesis in the hydroxide medium is closely similar to a convenient synthesis for pure silica ITQ-1 (MWW),[6] but has a lower pH due to the use of HMI as a hydrochloride salt. In a typical preparation, 3.50 g of HMI:HCl was dissolved in 19.86 g of H_2O before addition of 50.50 g of a solution of *N*,*N*,*N*-trimethyl-1-adamantammonium (0.412 mol/1000 g) and 5.01 g of silica (Aerosil 200). The mixture (pH = 11.2) was stirred for 2 h before being poured into Teflon-lined autoclaves, which were heated at 150 °C under slow rotation (60 rpm). Pure silica MCM-35 was obtained after 17 days of heating.

For the syntheses in the fluoride media, HMI was the only organic additive. HMI, silica, and water were mixed and stirred for 1 h before addition of either HF (aqueous) or a solution of NH_4F. When seeds were used, they were added after addition of the fluoride source in the form of a suspension of MCM-35 crystals in water, and the mixture was stirred further. In a typical synthesis of MCM-35 using seeds, 3.30 g of HMI, 10.01 g of Ludox AS-40, and 5.75 g of H_2O were stirred

* Corresponding author.

(1) Meier, W. M.; Olson, D. H.; Baerlocher, Ch. *Atlas of Zeolite Structure Types*, 4th ed.; Elsevier: Amsterdam, 1996.

(2) Davis, M. E.; Zones, S. I. in *Synthesis of Porous Materials. Zeolites, Clays and Nanostructures*; Occelli, M. L., Kessler, H., Eds.; Marcel Dekker: New York, 1997; p 1.

(3) Lobo, R. F.; Zones, S. I.; Davis, M. E. *J. Inclusion Phenom. Mol. Recogn. Chem.* **1995**, *21*, 47. Kubota, Y.; Helmkamp, M. M.; Zones, S. I.; Davis, M. E. *Microporous Mater.* **1996**, *6*, 213.

(4) Leonowicz, M. E.; Lawton, J. A.; Lawton, S. L.; Rubin, M. K. *Science* **1994**, *264*, 1910.

(5) Rubin, M. K., U.S. Patent 4,981,663, 1991.

(6) Camblor, M. A.; Corma, A.; Díaz-Cabañas, M. J.; Baerlocher, Ch. *J. Phys. Chem. B* **1998**, *102*, 44.

10.1021/cm9910660 CCC: $18.00
Published on Web 09/18/1999

Table 1. Synthesis Results

synthesis mixture							
$TMAdaOH/SiO_2$	HMI/SiO_2	F^-/SiO_2	H_2O/SiO_2	temp (°C)	time (days)	final pH	product (XRD)
0.25	0.31 (HMI:HCl)	−	44	150	2	9.7	amorphous
					3	10.4	amorphous
					7	9.1	amorphous
					14	10.1	MCM-35
					17	9.1	MCM-35
0.25	0.31	−	44	150	3	11.4	ITQ-1
					5	11.8	ITQ-1
					7	11.2	ITQ-1
					9	10.7	ITQ-1
					14	10.9	ITQ-1
					28	10.5	ITQ-1 + nonasil
					45	10.9	nonasil
−	0.31	−	44	150	14	10.5	amorphous
−[a]	0.31	−	44	150	14	12.7	quartz
−	0.50	0.50 (NH_4F)	7.5	150	7	10.7	amorphous
					14	9.6	nonasil + amorphous
					21	9.3	nonasil + MCM-35
−	0.50	0.50 (NH_4F)	15	150	6	9.4	amorphous + MCM-35
					7	10.2	MCM-35
					14	10.2	MCM-35
−	0.50	0.50 (NH_4F)	15	175	7	9.6	MCM-35
					12	10.2	MCM-35
−	0.50	0.50 (HF)	15	175	7	8.8	MCM-35
					12	8.9	MCM-35

[a] NaOH was added to this synthesis mixture ($NaOH/SiO_2 = 0.25$) to maintain the hydroxide content equal to that of the experiments performed in the presence of $TMAda^+$.

for 1 h. Then 1.23 g of NH_4F in 2.0 g of H_2O was added and a milky mixture was obtained. An ultrasonicated dispersion of 0.20 g of MCM-35 in 4.25 g of H_2O was then added. The resultant mixture (pH 10.4) was transferred to Teflon-lined autoclaves and heated at 175 °C under slow rotation (60 rpm). After 12 days of heating the solid formed was MCM-35 (this sample was used, after calcination, for the structure solution and refinement). In all cases, the solids were recovered by filtration, washed with deionized water, and dried at 100 °C.

Phase purity and crystallinity were determined by conventional powder X-ray diffraction (XRD) using a Philips PW1829 or X'Pert diffractometer (Cu Kα radiation, graphite monochromator) provided with a variable divergence slit and working in the fixed irradiated area mode. C, H, and N contents were determined with a Carlo Erba 1106 elemental organic analyzer. The fluoride content was determined[7] using an ion-selective electrode connected to a Mettler Toledo 355 ion analyzer. MAS NMR spectra of the solids were recorded on a Varian VXR 400SWB spectrometer. The ^{29}Si MAS NMR spectra were recorded with a spinning rate of 5.5 kHz at a ^{29}Si frequency of 79.459 MHz with a 55.4° pulse length of 4.0 μs and a recycle delay of 240 s. The $^1H-^{13}C$ CPMAS NMR spectra were acquired with a spinning rate of 5 kHz at a ^{13}C frequency of 100.579 MHz with a 90° pulse length of 7.5 μs, a contact time of 5000 μs and a recycle delay of 2 s. Both ^{29}Si and ^{13}C chemical shifts are reported relative to TMS. N_2 adsorption/desorption experiments were performed isothermally at 77 K using an automatic ASAP 2000 Micromeritics apparatus. High-resolution XRD data of a calcined MCM-35 sample prepared in the fluoride medium using seeds (see above) were recorded on station 2.3 of the Daresbury SRS in flat plate mode using the parameters summarized in Table 2.

Table 2. Data Collection and Crystallographic Parameters for the Title Compound

wavelength	1.400131 Å
temperature	298 K
2θ range	4−90° (range used 6−80°)
step size	0.01° 2θ
count time	4−50° 2θ 1 s/p 50−90° 2θ 2 s/p
number of data points	7400
number of reflections	893
number of profile parameters	17
number of structural parameters	55
number of constraints	0
unit cell	
a	9.49998(18) Å
b	30.7096(7) Å
c	7.31333(11) Å
β	91.7113(13)°
space group	$C12/m1$ (No. 12)
residuals	
R_{exp}	6.12
R_{wp}	9.16
R_p	7.29
R_b	3.02
χ^2	2.262

Results

Synthesis. Its is interesting that MCM-35 can be synthesized in the hydroxide media under conditions very similar to those conveniently yielding the much less dense zeolite ITQ-1.[6] Apparently, the use of HMI as a hydrochloride salt (which upon its hydrolysis will lower the pH of the synthesis media) favors the formation of MCM-35. Thus, when HMI is used, the final synthesis pH is around 11 and ITQ-1 fully crystallizes in 3 days. By contrast, when HMI:HCl is used, the final synthesis pH is below 10.5, no crystalline product appears during the first week of heating at 150 °C, and MCM-35 is fully crystallized in 2 weeks. A tentative rationalization of these observations for syntheses in the presence of both HMI and $TMAda^+$ (which afford together a good stabilization of the dual pore system of zeolite ITQ-1)[6] can be put forward based strictly on considerations of the pH. A high synthesis pH presumably produces a higher concentration of soluble silicate species (a higher supersaturation), which favors the formation of the less dense and presumably less stable ITQ-1, while at the lower pH the nucleation of that metastable phase is hindered and the more dense and stable MCM-35 is

(7) Guth, J. L.; Wey, R. *Bull. Soc. Fr. Minéral. Cristallogr.*, **1969**, *92*, 105.

obtained after prolonged heating. There is another plausible explanation based on the peculiar character of the ITQ-1 structure,[6] which in the as-synthesized form is a layered phase that is probably held together by the interaction between SiO^- groups and $TMAda^+$ cations. Since a low pH would favor protonation of the silanolates, a low pH may be detrimental to the formation of ITQ-1. We note, however, that at this stage both explanations are speculative attempts to rationalize our observations. It is interesting in this respect that the patent report on MCM-35 also describes the reaction mixture as "of low alkalinity".[5] When no $TMAda^+$ is added and HMI is used as a free amine, an amorphous phase is obtained after 2 weeks of heating, while if TMAdaOH is replaced by the equivalent amount of NaOH, quartz crystallizes after the same heating time. In the patent report, which makes use of HMI and NaOH or KOH (with M/SiO_2 typically in the 0.05−0.30 range, M being Na or K), only aluminosilicate MCM-35 materials are reported (with Si/Al in the 20−60 molar range).[5]

In a second synthetic route, also at relatively low pH, MCM-35 was crystallized using HMI and fluoride anions in the absence of $TMAda^+$ at 150 and 175 °C. At the lowest crystallization temperature, increasing the concentration of reagents (by lowering the H_2O/SiO_2 ratio) affords a less dense, though nonporous phase (NON, FD = 19.3 Si/1000 Å^3)[1] to crystallize first, although after further heating MCM-35 also crystallizes. This appears to be the usual trend for the synthesis of pure silica zeolites in the presence of fluoride:[8,9] when several phases are able to crystallize in the presence of a given organic additive, the less dense phase is frequently favored at the most concentrated conditions, while increasing the crystallization time or the temperature favors the most dense phase. This has been rationalized as a kinetic effect assuming that, generally, the less dense phase is thermodynamically less stable and needs to be crystallized under the conditions of (presumably) higher supersaturation.[9] Finally at 175 °C, MCM-35 crystallizes in 1 week using either NH_4F or HF as a source of F^- anions.

Characterization. Figure 1 shows the XRD patterns of several MCM-35 materials prepared in this work, each one corresponding to the best sample obtained under the different conditions (Table 1). The sample prepared in hydroxide media using TMAdaOH and HMI:HCl shows broad reflections and a poorly resolved pattern. The patterns of the samples prepared using HMI and NH_4F are better resolved and show sharper reflections, especially the one prepared at 175 °C using MCM-35 seeds. We believe these effects are mainly due to the crystallite size (Figure 2), since all the samples present a platelet morphology with the smallest dimension being thinner in the sample prepared in the hydroxide media and thicker in the fluoride samples (this is especially true when the temperature is increased to 175 °C and seeds are used).

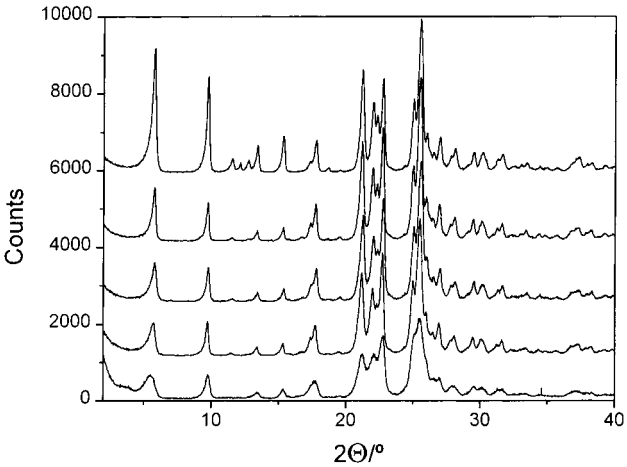

Figure 1. XRD patterns of the MCM-35 materials prepared (from bottom to top) in hydroxide medium using TMAdaOH and HMI:HCl; in fluoride medium using NH_4F at 150 °C; using HF at 175 °C; using NH_4F and MCM-35 seeds at 175 °C; and the same sample after calcination at 700 °C, 4 h (the sample used for the structure analysis). Note the dependence of peak broadening on preparation method.

The chemical composition of an MCM-35 material obtained using HMI and NH_4F at 175 °C and seeds indicates that there are two HMI molecules per unit cell of 44 SiO_2 tetrahedra (see structure below): 1.03% N, 5.63% C, 1.00% H, 0.20% F. The C/N ratio (6.5) is close to the ratio in HMI, suggesting the integrity of the occluded organics. This is further confirmed by ^{13}C CPMAS NMR experiments (Figure 3), which reveal that HMI is occluded intact in MCM-35 and is mainly in its unprotonated form. Only a small resonance at around 10 ppm and a broad one near 46 ppm suggest the presence of a minor concentration of protonated amine. This conclusion also agrees with the rather low F content (0.20%) and F/N ratio (0.15) when compared to typical silica materials prepared in fluoride media using alkylammonium cations (typically around 2% F by weight and around $F/N^+ = 1$).[10] The F content is slightly enhanced if HF is used instead of NH_4F (up to 0.30 F wt %), as a consequence of the lower synthesis pH (Table 1).

When MCM-35 is calcined at 700 °C for 4 h, a white solid with a high crystallinity is obtained (Figure 1, top), and N_2 adsorption reveals this template-free solid to contain microporosity (Figure 4). Very interestingly, the adsorption properties of the samples prepared in the hydroxide and fluoride media are very different, as shown in Figure 4. The N_2 adsorption isotherm of the sample prepared in the hydroxide medium is never flat, being very steep at high relative pressures and showing a clear hysteresis loop. All these observations suggest significant interparticle adsorption and are also present but in a much smaller degree in the isotherm of the fluoride sample. The micropore volume (measured by the *t*-plot method) of the sample prepared in hydroxide medium (0.027 cm^3/g) is only 40% of the volume found for the fluoride sample (0.070 cm^3/g). This does not appear to be due to differences in crystallinity (presence of amorphous material in the hydroxide sample) since the difference in the XRD peak areas in the 20−29° 2θ

(8) Barrett, P. A.; Boix, E. T.; Camblor, M. A.; Corma, A.; Díaz-Cabañas, M. J.; Valencia, S.; Villaescusa, L. A. In *Proccedings of the 12th International Zeolite Conference*; Treacy, M. M. J., Marcus, B. K., Bisher, M. E., Higgins, J. B., Eds.; Materials Research Society: Warrendale, 1998; p 1495.

(9) Camblor, M. A.; Villaescusa, L. A.; Díaz-Cabañas, M. J. *Topics Catal.* **1999**, *9*, 59.

(10) Koller, H.; Wölker, A.; Villaescusa, L. A.; Díaz-Cabañas, M. J.; Valencia, S.; Camblor, M. A. *J. Am. Chem. Soc.* **1999**, *121*, 3368.

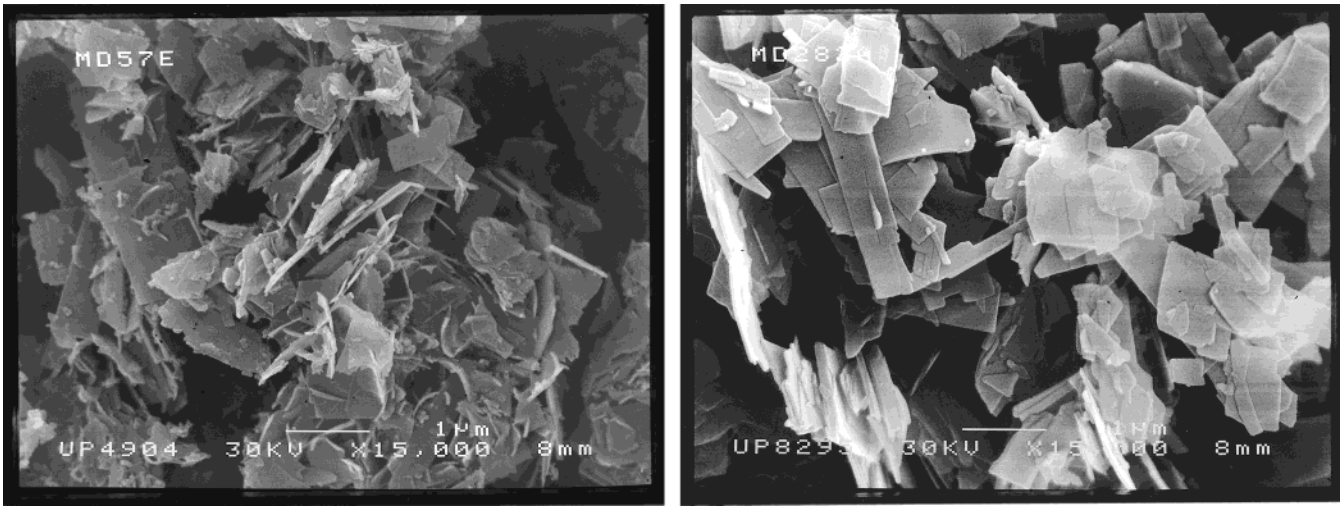

Figure 2. SEM micrographs of MCM-35 prepared in hydroxide (left) and fluoride medium (right, synthesized using NH_4F and seeds).

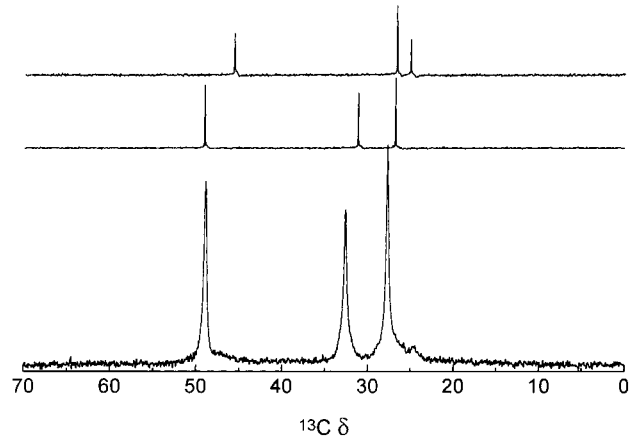

Figure 3. ^{13}C CPMAS NMR spectrum of as-made MCM-35 prepared using NH_4F and seeds (bottom); ^{13}C NMR of HMI (middle) and HMI:HCl (top) in $CDCl_3$ solution.

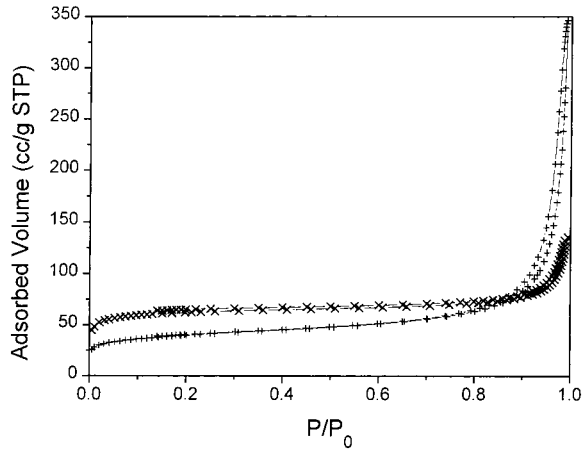

Figure 4. N_2 adsorption/desorption isotherms at 77 K of calcined MCM-35 materials prepared in hydroxide (+) and fluoride media (×). The differences between both isotherms are attributed to differences in crystal size along [010] (see the text and SEM of the same samples in Figure 2).

region is smaller than 15% for both samples and the ^{29}Si MAS NMR spectra rules out the presence of significant amounts of amorphous silica. The presence of connectivity defects cannot explain this observation either (see below).

The reason for the observed difference in micropore volume and in the shape of the isotherms is probably related to crystal size and morphology. XRD peak broadening of (0*k*0) reflections and platelike preferred orientation normal to [010] (see below) suggest that the large face of the plates shown in Figure 2 are the (010) faces. Considering the crystal structure described below, the channels run parallel to these faces. If the crystallites terminate after completion of the dense layers that separate the channels (see structure below), then variations of the small dimension of the crystallites (along [010]) will significantly alter the micropore volume because crystal termination normal to (010) "converts" some microporous surfaces into external surfaces. Thus, in short, the thinner the crystallites are, the smaller the micropore volume is. The effect of nanocrystallinity of zeolites on the observed micropore volume was recently illustrated for the case of zeolite Beta,[11] which possesses a three-dimensional channel system. In the case of MCM-35, the coupling of the platelet crystal morphology and the orientation of the one-dimensional channels normal to the short [010] dimension of the crystallites makes the micropore volume largely dependent on the size of the crystallites along [010]. This type of effect may well explain the striking differences in the adsorption properties of the MCM-35 materials reported in the patent, where 2-fold variations in the cyclohexane and *n*-hexane uptakes at 40 Torr are reported (1.7−3.4 and 2.2−4.7 wt %, respectively).

The material prepared in the fluoride medium using HMI as the unique organic additive presents, after calcination, the ^{29}Si MAS NMR shown in Figure 5. The spectrum shows a very small resonance around −100 ppm (≅1% of the total intensity), indicating that the material is essentially free of connectivity defects, and also a nice resolution of $Si(OSi)_4$ species in at least four different crystallographic sites. This is typical of pure silica materials prepared in fluoride media at near to neutral pH.[9] However, in the case of MCM-35, the pure silica material prepared in the absence of fluoride using TMAdaOH and HMI:HCl also presents a very small

(11) Camblor, M. A.; Corma, A.; Valencia, S. *Microporous Mesoporous Mater.* **1998**, *25*, 59.

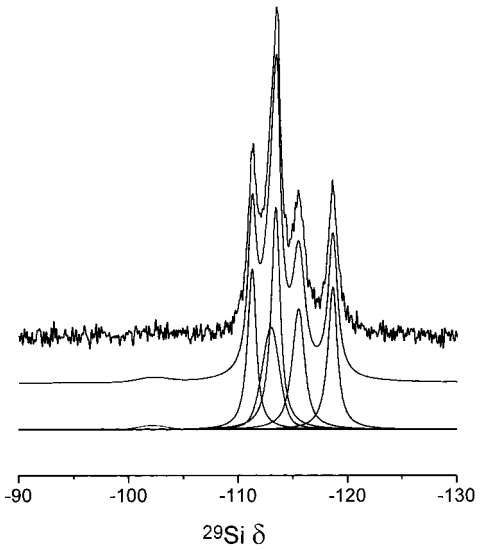

Figure 5. ^{29}Si MAS NMR spectrum of calcined SiO_2 MCM-35 prepared in the fluoride medium using seeds: experimental (top), simulation (middle), and deconvoluted components (bottom).

concentration of connectivity defects (around 4.4% Si-$(OSi)_3O$ defect groups). The absence of connectivity defects in SiO_2 materials prepared in fluoride media with organoammonium cations has been rationalized and attributed to several factors.[9] The most important ones are that charge balance of the occluded organic cations is accomplished by occluded fluoride,[10] instead of $Si-O^-$ groups, and that the low synthesis pH favors condensation of adjacent Si−OH groups through dehydration reactions. In the case of the MCM-35 material prepared in the hydroxide medium, but at relatively low pH, the reasons for the low concentration of defects may be similar: first, the organic additive is an amine and is probably incorporated mainly in its unprotonated uncharged form, thus not needing a large concentration of $Si-O^-$ defects for charge compensation; second, the synthesis pH is relatively low (9.1) and thus full condensation is favored. Deconvolution of the spectrum of the sample prepared in the fluoride medium in the region of $Si(OSi)_4$ species shows the presence of five resonances with approximate relative intensities 2:2:3:2:2 (Figure 5), consistent with our proposed structure (see below) which, in space group *C*2/*m*, contains six crystallographically distinct tetrahedral sites (multiplicities 4:8:8:8:8:8).

Structure Determination. All the peaks in the pattern of calcined MCM-35 were successfully indexed from laboratory-based XRD data. The unit cell was found to be monoclinic (approximate dimensions a = 9.49 Å, b = 30.71 Å, c = 7.31 Å, and β = 91.7°), and the systematic absences proved consistent with space groups *C*2/*m*, *Cm*, or *C*2. Le Bail[12] type profile fitting using the Mprofil[13] suite of programs revealed that the complete pattern could be matched with no traces of impurities found, although some peak broadening of the [0*k*0] reflections could be noted. The synchrotron XRD dataset was also examined with Le Bail[12] profile fitting as above before direct methods were attempted based on the intensities extracted in space group *C*2/*m* using the program Sirpow[14] from which a complete structural model was obtained.

Rietveld[15] refinement of the model produced by direct methods was then undertaken in the GSAS[16] code. A pseudo-Voigt[17] function was used to describe the peak shape together with, in the initial stages, a manually interpolated background. After the scale factor was refined, and then subsequently the lattice parameters and zero point, the profile parameters were allowed to vary. At this stage the first peak in the pattern ((020) reflection) was removed due to its considerable broadness and asymmetry, which could not acceptably be matched even by including peak broadening and asymmetry corrections available in GSAS.[16] The results from Le Bail[12] fitting showed that the rest of the pattern could be adequately fitted if corrections for asymmetry and broadening of the [0*k*0] reflections were included.[18] Soft constraints were then applied to the Si−O interatomic distances to allow the atomic positions and temperature factors to be refined. After a few cycles of refinement it became clear that the intensities of the [0*k*0] reflections could not be matched by small shifts in the atomic positions, suggesting in addition that a preferred orientation correction was necessary. We note that the crystallites have a very platelike morphology (Figure 2) and thus, given the fact that the data were collected in flat plate mode, preferred orientation is to be anticipated. The formulation of March and Dollase[19] available in GSAS[16] was applied. This not only improved the fit but also enabled the soft constraints to be removed. Finally a five-coefficient shifted Chebyshev[16] function was included to improve the fit to the background and the model fully refined to convergence. The final agreement factors are summarized together with the rest of the crystallographic parameters in Table 2, the Rietveld plot is shown in Figure 6, and the atomic positions and isotropic temperature factors are given in Table 3.

Throughout the refinement described above, in space group *C*2/*m* (No. 12), it was observed that one of the Si−O−Si angles (around O(19); see Table 4) remained uncharacteristically high (ca. 176°) for zeolite materials, suggesting this symmetry not to be wholly satisfactory. However, attempts to reduce the symmetry to *C*2 or *Cm* did not improve the fit significantly but at the same time increased considerably the number of parameters (in *C*2 the number of atoms in the asymmetric unit becomes 37 and in *Cm* 34). Examining this symmetry problem by energy minimization methods[20] using the GULP[21]

(12) Le Bail, A.; Duroy, H.; Fourquet, J. L. *Mater. Res. Bull.* **1988**, *23*, 447.
(13) Murray, A. D.; Fitch, A. N. *Mprofil Program for Le Bail Decomposition and Profile Refinement*, 1990.
(14) Atomare, A.; Burla, C.; Cascarano, C.; Giacovazzo, C.; Gualiardi, A.; Polidori, G.; Carnalli, M. *J. Appl. Crystallogr.* **1994**, *27*, 435.
(15) Rietveld, H. M. *J. Appl. Crystallogr.* **1969**, *2*, 65.
(16) Larson A.; Von Dreele, R. B. GSAS Manual, Los Alamos Report No. LA-UR-86-748, 1986.
(17) Hastings, J. B.; Thomlinson, W.; Cox, D. E. *J. Appl. Crystallogr.* **1984**, *17*, 85.
(18) We have investigated the possibility of intergrowths normal to [010] and found that MCM-35 can be intergrown with "decasil" structures (like RUB-3, see below). However, given the relation between broadening and particle size (see Figures 1 and 2 and the characterization section), we believe that broadening of the [0*k*0] reflections is mainly due to particle size effects.
(19) Dollase, W. A. *J. Appl. Crystallogr.* **1986**, *19*, 267.
(20) *Computer Simulation of Solids*; Catlow, C. R. A., Mackrodt, W. C., Eds.; Springer-Verlag: Berlin, 1982; vol 166.
(21) Gale, J. D. *J. Chem. Soc., Faraday Trans.* **1997**, *93*, 629.

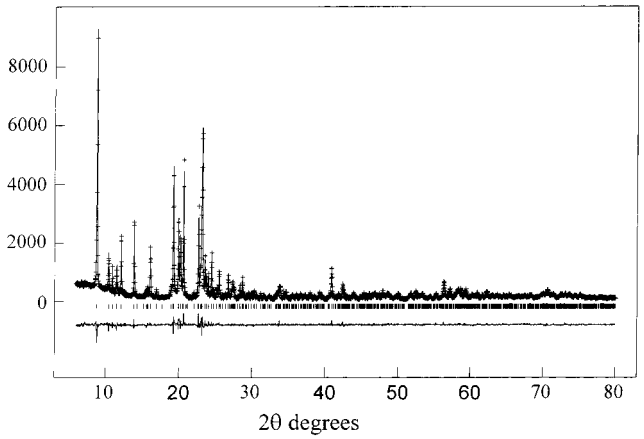

Figure 6. Observed (+) and calculated (solid line) X-ray diffraction patterns for calcined pure silica MCM-35 (wavelength 1.400131 Å) following Rietveld refinement. Vertical ticks indicate the positions of allowed reflections in space group *C*2/*m*. The lower trace is the difference plot.

Table 3. Atomic Positions and Isotropic Temperature Factors for Calcined MCM-35 in *C*2/*m* Symmetry with esd's in Parentheses

atom	*x*	*y*	*z*	U_{iso} (Å^2)[1]
Si(1)	0	0.08356(23)	0	0.0052(24)
Si(2)	0.1910(6)	0.15359(17)	−0.1667(8)	0.0158(18)
Si(3)	−0.0048(6)	0.22858(17)	−0.2913(5)	0.0037(18)
Si(4)	−0.1271(5)	0.04862(17)	−0.3710(6)	0.0092(17)
Si(5)	−0.3049(6)	0.19803(17)	−0.1822(7)	0.0060(17)
Si(6)	−0.3391(5)	0.12303(15)	−0.4749(7)	0.0031(17)
O(7)	−0.0756(10)	0.05227(30)	−0.1609(12)	0.0205(10)
O(8)	−0.5	0.10684(40)	−0.5	0.0205(10)
O(9)	0	0.23506(38)	−0.5	0.0205(10)
O(10)	0	0.06345(39)	−0.5	0.0205(10)
O(11)	0.2923(8)	0.17606(28)	−0.0075(14)	0.0205(10)
O(12)	−0.2593(9)	0.08102(30)	−0.4062(11)	0.0205(10)
O(13)	0.0624(11)	0.26900(34)	−0.1981(12)	0.0205(10)
O(14)	0.1281(9)	0.11111(27)	−0.0804(13)	0.0205(10)
O(15)	−0.2807(9)	0.13899(28)	−0.6705(14)	0.0205(10)
O(16)	0.0798(11)	0.18695(30)	−0.2331(13)	0.0205(10)
O(17)	−0.1766(12)	0	−0.4029(16)	0.0205(10)
O(18)	−0.1646(11)	0.22635(32)	−0.2230(11)	0.0205(10)
O(19)	−0.3268(9)	0.16144(31)	−0.3269(12)	0.0205(10)

[a] Note that the temperature factors for the oxygen atoms were refined so as to be equal.

code and silicate potentials of Sanders et al.[22] showed us that the results (lattice energies, atomic positions, and cell parameters) for calculations in space groups *C*2/*m* and subgroups *C*2 and *Cm* were very similar. However, we found that when space group $P2_1/c$ was tried, the results were almost identical to those obtained when the symmetry was switched off before the structure was optimized ("no symmetry"). In the other symmetries tested in this way (*C*2/*m* and subgroups *C*2 and *Cm*), the calculated lattice energies were slightly less favorable, and particularly, the unit cell volumes obtained after minimization were larger than the "no symmetry" and $P2_1/c$ minimized structures (see Table 5). This would suggest from the viewpoint of minimization that in space groups *C*2/*m*, *C*2, and *Cm* the structures are constrained too much and thereby the unit cell volume is unable to reduce to the level found for the no symmetry and $P2_1/c$ optimized lattices. Subsequent attempts to refine the structure in $P2_1/c$ were made without much success. It was found that with 33 atoms needed in the asymmetric unit in this symmetry soft constraints on the Si−O distances had to be used. With this added limitation the fit observed was not found to be significantly better than that obtained earlier in *C*2/*m*, and the esd's showed in all cases that the refined parameters were less reliable. With this in mind we have maintained our model in *C*2/*m*, where the connectivity of this new structure can clearly be discerned, but we point out that the true symmetry may well be closer to $P2_1/c$, as suggested by energy minimization.

(22) Sanders, M. J.; Leslie, M.; Catlow, C. R. A. *J. Chem. Soc. Chem Commun.* **1984**, 1271.

Table 4. Selected Bond Distances and Angles for Calcined MCM-35 with esd's in Parentheses

bond (Å)		angle (deg)	
Si(1)−O(7)	1.665(9)	O(7)−Si(1)−O(7)	109.5(8)
Si(1)−O(7)	1.665(9)	O(7)−Si(1)−O(14)	111.1(4)
Si(1)−O(14)	1.608(8)	O(7)−Si(1)−O(14)	104.3(4)
Si(1)−O(14)	1.608(8)	O(7)−Si(1)−O(14)	104.3(4)
		O(7)−Si(1)−O(14)	111.1(4)
		O(14)−Si(1)−O(14)	116.5(7)
Si(2)−O(11)	1.641(9)	O(11)−Si(2)−O(14)	106.6(6)
Si(2)−O(14)	1.575(9)	O(11)−Si(2)−O(15)	110.0(6)
Si(2)−O(15)	1.551(9)	O(11)−Si(2)−O(16)	109.1(5)
Si(2)−O(16)	1.540(9)	O(14)−Si(2)−O(15)	107.0(5)
		O(14)−Si(2)−O(16)	114.4(6)
		O(15)−Si(2)−O(16)	109.7(7)
Si(3)−O(9)	1.541(4)	O(9)−Si(3)−O(13)	108.0(6)
Si(3)−O(13)	1.545(11)	O(9)−Si(3)−O(16)	110.2(6)
Si(3)−O(16)	1.562(10)	O(9)−Si(3)−O(18)	111.6(5)
Si(3)−O(18)	1.614(9)	O(13)−Si(3)−O(16)	109.6(5)
		O(13)−Si(3)−O(18)	106.1(6)
		O(16)−Si(3)−O(18)	111.2(7)
Si(4)−O(7)	1.602(8)	O(7)−Si(4)−O(10)	109.1(5)
Si(4)−O(10)	1.619(5)	O(7)−Si(4)−O(12)	108.9(6)
Si(4)−O(12)	1.617(10)	O(7)−Si(4)−O(17)	106.8(7)
Si(4)−O(17)	1.581(6)	O(10)−Si(4)−O(12)	108.9(5)
		O(10)−Si(4)−O(17)	113.8(8)
		O(12)−Si(4)−O(17)	109.3(6)
Si(5)−O(11)	1.544(9)	O(11)−Si(5)−O(13)	112.2(6)
Si(5)−O(13)	1.618(10)	O(11)−Si(5)−O(18)	110.9(6)
Si(5)−O(18)	1.627(10)	O(11)−Si(5)−O(19)	107.5(6)
Si(5)−O(19)	1.553(10)	O(13)−Si(5)−O(18)	107.0(6)
		O(13)−Si(5)−O(19)	108.4(6)
		O(18)−Si(5)−O(19)	110.8(5)
Si(6)−O(8)	1.613(6)	O(8)−Si(6)−O(12)	103.3(6)
Si(6)−O(12)	1.571(8)	O(8)−Si(6)−O(15)	109.9(5)
Si(6)−O(15)	1.626(10)	O(8)−Si(6)−O(19)	110.7(5)
Si(6)−O(19)	1.603(9)	O(12)−Si(6)−O(15)	110.8(5)
		O(12)−Si(6)−O(19)	111.3(6)
		O(15)−Si(6)−O(19)	110.7(5)
		Si(1)−O(7)−Si(4)	146.2(7)
		Si(6)−O(8)−Si(6)	144.1(10)
		Si(3)−O(9)−Si(3)	165.2(10)
		Si(4)−O(10)−Si(4)	147.3(10)
		Si(2)−O(11)−Si(5)	148.2(7)
		Si(4)−O(12)−Si(6)	157.1(7)
		Si(3)−O(13)−Si(5)	147.7(7)
		Si(1)−O(14)−Si(2)	152.0(7)
		Si(2)−O(15)−Si(6)	166.5(7)
		Si(2)−O(16)−Si(3)	166.6(7)
		Si(4)−O(17)−Si(4)	141.7(10)
		Si(3)−O(18)−Si(5)	149.7(7)
		Si(5)−O(19)−Si(6)	176.4(8)

Table 5. Lattice Energy Minimization Results for MCM-35 at Constant Pressure

space group	lattice energy (eV)	difference (eV)	unit cell volume (Å^3)	difference (Å^3)
*P*1	−2829.70		2032.09	
*C*2/*m*	−2829.53	−0.17	2072.91	40.82
*C*2	−2829.53	−0.17	2072.78	40.69
Cm	−2829.58	−0.12	2056.04	23.95
$P2_1/c$	−2829.70	0	2032.09	0

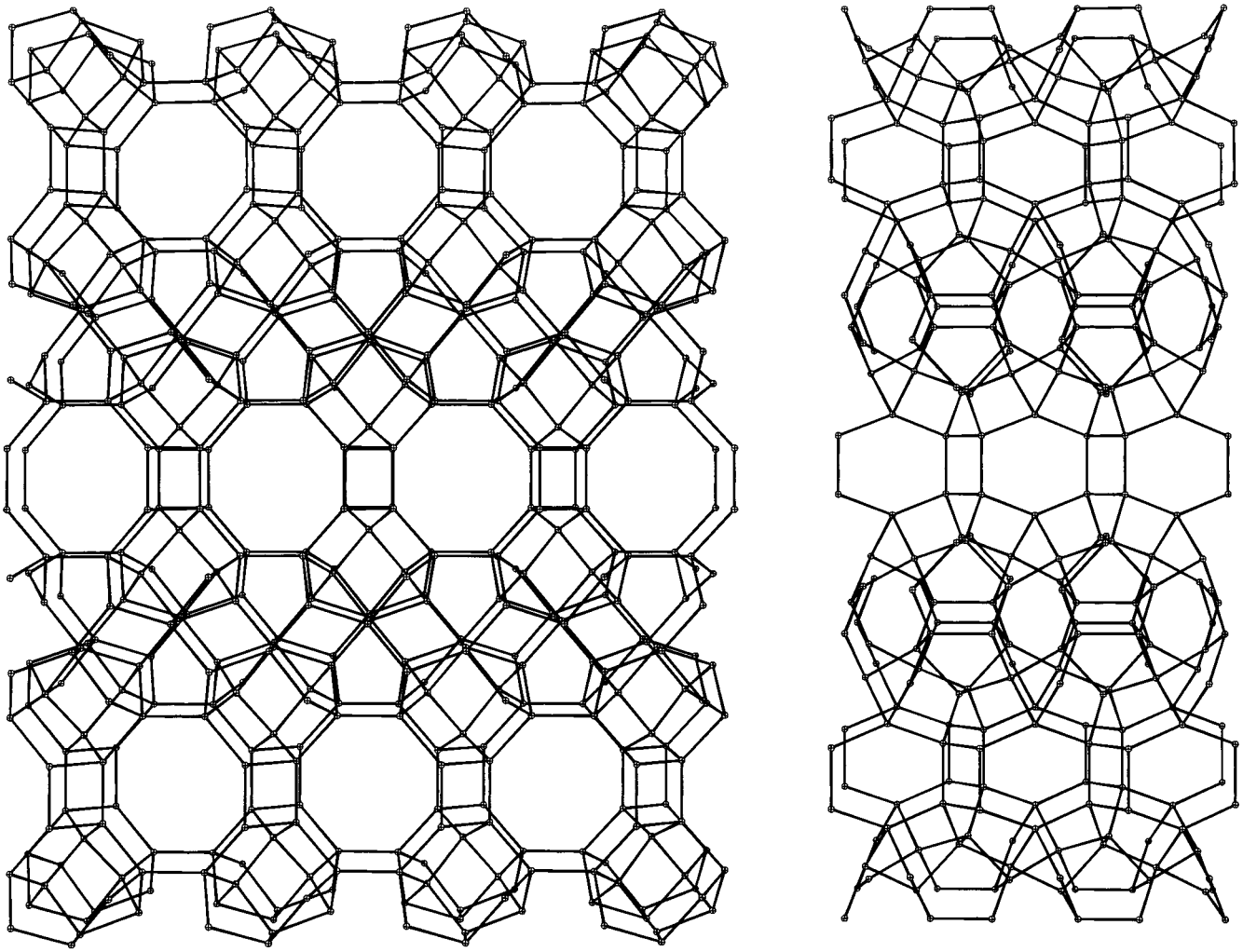

Figure 7. The framework topology of MCM-35 in perspective views along [001] (left) and [100] (right). Only the tetrahedral connectivity is shown. Note that the only 4MR in MCM-35 are those that separate two adjacent 8MR channels (i.e., those linking the very dense layerlike portions of the structure).

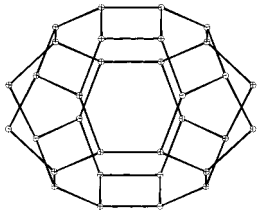

Figure 8. The $[4^2 5^8 6^2 8^4]$ cage of zeolite MCM-35. The 8MR windows at the top and at the bottom of the cage define the 8MR channel. By contrast, the very puckered and elongated 8MR windows at each side of the cage face very dense portions of the structure and, thus, do not form a zeolitic channel.

Description of the MCM-35 Structure. MCM-35 has a unique four-connected, three-dimensional SiO_2 framework containing one-dimensional channels running along [001] (Figure 7). These channels have 8MR windows as minimum constricting apertures (free crystallographic dimensions 3.55 × 4.17 Å). Between the 8MR windows there is a wider $[4^2 5^8 6^2 8^4]$ cage, depicted in Figure 8, and the channels may be viewed as a piling of such cages along [001].[23] It is interesting that MCM-35 has portions of relatively low density, with adjacent 8MR channels separated in the [100] direction by single 4MR and 6MR, while other portions have very high density. Thus, the structure may be formally viewed as composed of very dense layers normal to [010] that are joined to each other through 4MR, giving rise to the 8MR channels. It is possible to define a fundamental building unit for MCM-35 which consists of a small cage composed of eight 5MR, $[5^8]$. These units are linked to each other along z by sharing two edges, thus forming a chainlike building unit (Figure 9). Each chain cross-links to four adjacent chains in a rather complex way to yield the dense layers mentioned above.[24]

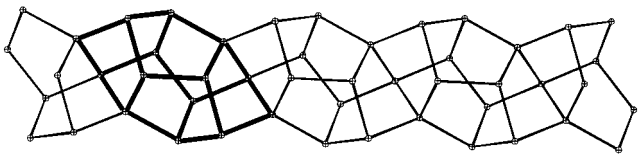

Figure 9. The chainlike building block of MCM-35 with a single $[5^8]$ polyhedron highlighted.

(23) In the notation $[m^n...]$, polyhedra are defined by the n number of faces with m Si−O−Si edges.

(24) Note that this is just a formal description of the structure of MCM-35 and that, unlike MWW materials (see ref 6, for instance), as-made MCM-35 already shows the four-connected three-dimensional topology described here for the calcined material (even when dried at room temperature).

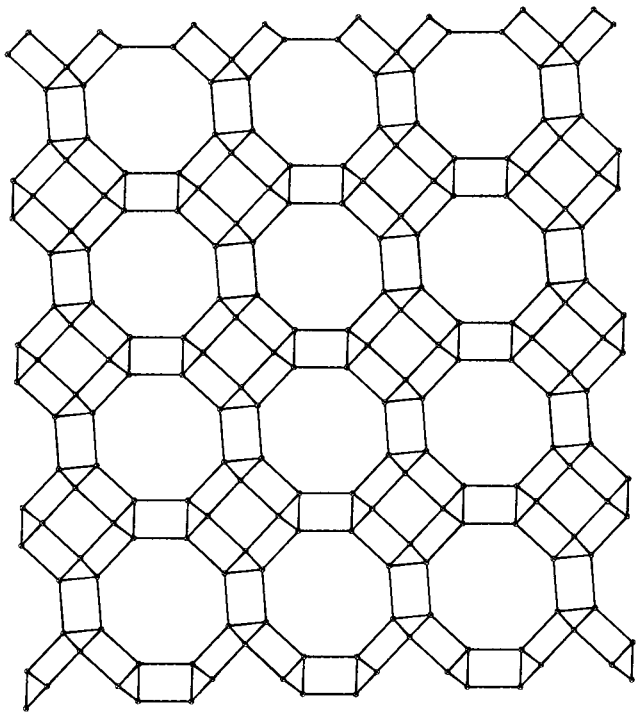

Figure 10. The framework topology of RUB-3 (RTE)[26] in projection along the channels.

Interestingly, MCM-35 appears to be related to the family of the so-called "decasil zeolites" discovered by Marler et al.[25] The projection along the channels of MCM-35 and the decasils show striking similarities, as can be seen by comparing Figures 7 and 10 (RUB-3, structure code RTE,[26] which is decasil A). We should note, however, that while the decasils have a relatively large concentration of 4MR (Figure 10), most features looking like 4MR in Figure 7 are merely an artifact of the projection. The only 4MR in MCM-35 are those linking the dense layerlike portions of the structure. The $[4^2 5^8 6^2 8^4]$ cage of MCM-35 (Figure 8) also resembles the $[4^6 5^4 6^6 8^2]$ and $[4^4 5^8 6^4 8^2]$ cages of the decasil structures.[25] However, MCM-35 cannot be built using the fundamental unit of the decasils (a $[4^4 5^4 6^2]$ decahedron). More importantly, all the decasils (real or hypothetical)[25] previously proposed lack the very dense layers that separate the channels of MCM-35 in the [010] direction, as referred to above. Due to this, the reported decasils are far less dense than MCM-35, although all of them present one-dimensional 8MR channels. For instance, the framework density of RTE (decasil A) is 17.3 Si/nm^3, while the value for MCM-35 is 20% larger (20.6 Si/nm^3). Actually, the framework density of MCM-35 is the largest known for zeolites (only equaled by that of the cesium aluminosilicate CAS).[1]

MCM-35, RUB-3, and RUB-4 (a disordered member of the decasil family)[25,27] are the only known pure silica materials containing one-dimensional 8MR channels. Their synthesis share in common the use of cyclic amines as structure-directing agents. However, while MCM-35 is synthesized with a monocyclic, and thus relatively flexible, amine (HMI), RUB-3 and RUB-4 are synthesized with bulkier and more rigid bicyclic amines (*exo*-2-aminobicyclo[2.2.1]heptane and 3-azabicyclo[3.2.2]-nonane, respectively)[25] for which a greater conformational rigidity and, hence, a greater specificity in the structure-direction can be anticipated.

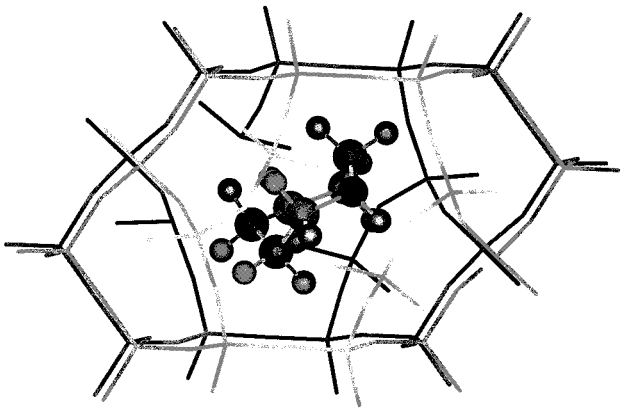

Figure 11. The approximate location of the hexamethyleneimine molecule inside the $[4^2 5^8 6^2 8^4]$ cage of zeolite MCM-35, according to docking calculations. Note that the cage has been rotated with respect to Figure 8 to show its diagonal elongation. See the text for details.

SDA Docking Studies. The size and shape of the hexamethyleneimine SDA compared to the void system of MCM-35 suggested to us that the SDA is probably localized in the as-made material inside the $[4^2 5^8 6^2 8^4]$ cage (Figure 8). A similar situation most likely occurs for the aminobicycloheptane SDA in the decasil RTE.[26] We note that the HMI content in MCM-35 (see above) points to a complete filling of the cages (2/uc). We thus decided to investigate if there may be a certain degree of correlation between the size and shape of the SDA and the size and shape of the cage in which it is probably located, to shed some light on the structure-directing ability of HMI during the crystallization of this unusual zeolite topology. We undertook a molecular modeling approach to dock into the purely siliceous host the template by Monte Carlo means before applying energy minimization methods to optimize these crudely loaded guest molecules. The methodology applied (including the potential force field) has been widely used for this type of study and has been fully described elsewhere.[28] The results of the docking calculations[29] show that the template moiety does not adopt a planar location parallel to the eight-membered ring windows but prefers to lie inclined to this aperture, expanding itself along the elongated diagonal of the cage (see Figure 11). In all cases this proved to be the optimum location. However, some disorder was observed from these calculations, manifesting itself by means of a rotation of the HMI molecule, which maintains the general location of the template ring but prevents discrimination of the different atom types. This loose match between the diagonally elongated shape of the cage and the orienta-

(25) Marler, B.; Grünewald-Lüke, A.; Gies, H. *Zeolites* **1995**, *15*, 388.

(26) Marler, B.; Grünewald-Lüke, A.; Gies, H. *Microporous Mesoporous Mater.* **1998**, *26*, 49.

(27) Gies, H.; Kirchner, R.; van Koningsveld, H.; Treacy, M. M. J. In *Proccedings of the 12th International Zeolite Conference*; Treacy, M. M. J., Marcus, B. K., Bisher, M. E., Higgins, J. B., Eds.; Materials Research Society: Warrendale, 1998; p 2999.

(28) Freeman, C. M.; Catlow, C. R. A.; Thomas, J. M.; Brode, S. *Chem. Phys. Lett.* **1991**, *186*, 137. Freeman, C. M.; Catlow, C. R. A.; Lewis, D. W. *J. Phys. Chem.* **1995**, *99*, 11194.

(29) InsightII v235 and Discover v295, Biosym Technologies Inc., San Diego, 1995.

tion of the SDA may be of importance in understanding the crystallization of MCM-35.[30]

Acknowledgment. The authors greatly acknowledge financial support by the Spanish CICYT (project MAT97-0723). We thank the CLRC for provision of the synchrotron radiation facilities and Dr. C. Tang for assistance with the data collection. P.A.B. is grateful to the European Union TMR program for a postdoctoral fellowship.

(30) Note added in proof: The framework topology of zeolite MCM-35 has been assigned the structure code MTF by the Structure Commission of the International Zeolite Association.

CM9910660